

# Calibration of TDR probes for water content measurements in partially saturated pyroclastic slope

A.S. Dias

*Department of Civil, Architectural and Environmental Engineering, University of Naples Federico II, Italy; Amap, Inra, Ird, Cnrs, Cirad, University of Montpellier, France*

M. Pirone & G. Urciuoli

*Department of Civil, Architectural and Environmental Engineering, University of Naples Federico II, Italy*

**ABSTRACT:** Monitoring of water content in partially saturated slopes prone to landslide could be essential for the good functioning of an early warning system. In this regard, Campania region in Southern Italy is an area with an extensive record of rainfall-induced landslides. In Western Campania, slopes consist of pyroclastic soil cover in partially saturated conditions resting on limestone. Time-domain reflectometry (TDR) allows monitoring of the soil dielectric constant, which is related to the volumetric water content. Topp et al. (1980) proposed the most popular relation between these two parameters but it does not provide satisfactory results when applied to volcanic soils. Therefore, when dealing with pyroclastic soil, ad hoc calibration is required. Here, the calibration of TDR probes in undisturbed pyroclastic soil samples collected at the Mount Faito test site (Campania, Italy) is shown and the proper relation between volumetric water content and dielectric constant is proposed. Lastly, these calibration curves are compared to those found for other pyroclastic soils belonged to different geologic contexts in Campania.

## 1 INTRODUCTION

The Campania Region (Southern Italy) is frequently affected by flowslides induced by intense rainfall events. These landslides are shallow and characterized by a great destructive power (Hungri et al., 2014). Past events, as the ones of Sarno (in 1998) and Nocera (in 2004), caused great economic and human losses (Frattini et al., 2004; De Vita et al., 2006).

Slopes susceptible to the occurrence of landslides consist of a thin layer of pyroclastic soil (2 to 3 m) resting on fractured limestone bedrock. These slopes can be as steep as  $37^\circ$  to  $45^\circ$ ; in saturated condition, the soil friction angle of the soil involved varies between  $35^\circ$  and  $38^\circ$ . Therefore, the stability is only guaranteed by an apparent cohesion (due to suction), which decreases or vanishes with the occurrence of rainfall (Urciuoli et al., 2016).

The monitoring of such slopes has been proved essential for a proper study of the groundwater regime (Pirone et al., 2015a) and assessment of the safety of slopes (Pirone et al., 2015b).

Some popular methods to determine water content are gravimetric sampling, neutron scattering, gamma ray attenuation and time-domain reflectometry (Noborio, 2001). This paper is focused on the latest method, in particular it is shown how the dielectric constant (also known as relative permittivity) of pyroclastic soils sampled in the Mount Faito test site

( $40^\circ40'30.08''N$ ,  $14^\circ28'23.98''E$ ; Naples, Southern Italy) has been determined. Then, the results have been compared to those obtained by Papa and Nicoletta (2012) for pyroclastic soils sampled at the Monteforte Irpino test site ( $40^\circ54'13.11''N$ ,  $14^\circ40'24.21''E$ ; Avellino, Southern Italy), originated by a different volcanic eruption and belonging to a different basin. Finally, the possibility of using a unique calibration function for pyroclastic soil with the same grain size distribution is discussed.

## 2 PRINCIPLES OF TIME-DOMAIN REFLECTOMETRY

The dielectric constant is determined by the time-domain reflectometry (TDR). A pulse is sent through a coaxial cable, which is connected to the TDR probe. These probes have 2 or 3 rods to arrange a system equivalent to a parallel element transmission line. The signal is then reflected and detected by an oscilloscope. It depends on the presence of discontinuities, i.e. the geometry change from the cable to the probe, the variations of dielectric properties and the probe extremity (Reder et al., 2014).

The signal round-time ( $\Delta t$ ) is the travel time of an electromagnetic pulse along a metallic waveguide and it is given by Equation 1, where  $L$  is the probe length,  $K_a$  is the apparent dielectric constant and  $c$  is

the velocity of electromagnetic signals in free space ( $c=3 \times 10^8$  m/s).

$$\Delta t = \frac{2L\sqrt{K_a}}{c} \quad (1)$$

The dielectric constant of water relative to those of minerals is high. Consequently, changes in volumetric water content can be directly related to the change in the dielectric constant of bulk soil.

The apparent dielectric constant of the soil can be simplified as the ratio between the apparent probe length ( $L_a = c \Delta t/2$ ) and the real probe length (Equation 2).

$$K_a = \left(\frac{L_a}{L}\right)^2 \quad (2)$$

The soil dielectric properties are strongly dependent on the soil water content, but they are also affected by the soil-water salinity, soil texture, bulk density, mineralogy, organic matter content, and frequency (Hendrickx et al., 2003). Topp et al. (1980) proposed a “universal” relation between the soil volumetric water content and the dielectric constant (Equation 3). Another well-known empirical relation is the one of Ledieu et al. (1986) reported in Equation 4. However, studies have shown that those relations are unsatisfactory when applied to some types of soils, such as organic and volcanic soils, as mentioned by Papa and Nicotera (2012).

$$\theta = -5.3 \cdot 10^{-2} + 2.92 \cdot 10^{-2} K_a - 5.5 \cdot 10^{-4} K_a^2 + 4.3 \cdot 10^{-6} K_a^3 \quad (3)$$

$$\theta = 0.1138\sqrt{K_a} - 0.1758 \quad (4)$$

The particular dielectric behavior of soil of volcanic origin is due to the high dielectric constant values of the solid particles (closer to 15, while most vary between 3 and 10), and low bulk density, as mentioned by Comegna et al. (2013).

In general, the calibration function, such that proposed by Topp et al. (1980), are polynomial as Equation 5 or logarithmical as Equation 6, where  $a$ ,  $b$ ,  $c$  and  $d$  are calibration constants.

$$\theta = a \cdot K_a^3 + b \cdot K_a^2 + c \cdot K_a + d \quad (5)$$

$$\theta = a + b \cdot \ln K_a \quad (6)$$

Another type of approach consists of semi-empirical models that consider the dielectric constant of 3 or 4 phases. The 3-phase model proposed by Roth et al. (1990) is an example. It takes the form of Equation 7, where  $\epsilon_w$ ,  $\epsilon_s$  and  $\epsilon_a$  are the water, solid and air dielectric constants, respectively,  $n$  is the soil porosity and  $\alpha$  is a fitting parameter which ranges between -1 and 1. Here Equation 8 was used to determine the dielectric constant of the solid particles that depends on the specific gravity of the soil

( $\rho_s$ ) in  $\text{g/cm}^3$  (Dobson et al., 1985). The dielectric constants of water and air are respectively 80 at  $20^\circ\text{C}$  and 1.

$$\theta = \frac{K_a^\alpha - (1-n)\epsilon_s^\alpha - n \cdot \epsilon_a^\alpha}{\epsilon_w^\alpha - \epsilon_a^\alpha} \quad (7)$$

$$\epsilon_s = (1.01 + 0.44\rho_s)^2 - 0.062 \quad (8)$$

### 3 THE MOUNT FAITO TEST SITE

An extensive investigation in the test site on Mount Faito, part of the Lattari mountains in Campania Region (Southern Italy), is going on. The stratigraphy recognized at this site is mainly composed of three pyroclastic soil layers (named A, B and C, in Figure 1), originated from two different volcanic eruptions, resting on limestone. The first and most superficial layer (1 m thick) consists of the two pyroclastic soils, named respectively A1 and A2, that vary between silty sand with gravel and silty gravel with sand. Soil A2 has a greater fraction of gravel (pumeces). The second layer, named B (0.8-1 m thick) is composed of well-graded gravel (pumeces) and it is not analysed in this paper. Then, the third layer, referred as soil C, is classified as sandy silt.

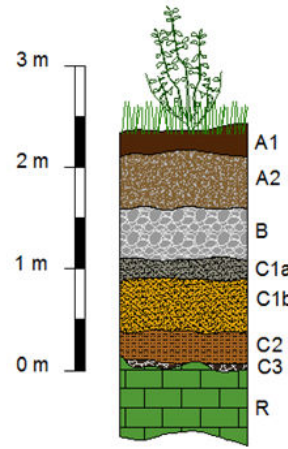


Figure 1. Stratigraphic profile in Mount Faito site.

The soil grain size distribution range of the first and third soil layers is represented in Figure 2, in which also a comparison with Monteforte Irpino soils is operated. The grain size curves of the surficial layer, soil 1 (0.4 m thick), soil 2 (0.4 m thick), and the deepest one, named soil 6 (located at 3 m from soil surface; 0.50 m thick) sampled at the Monteforte Irpino test site (Pirone et al., 2015a), are overlapped to those of Mount Faito soil A1, A2 and C1, respectively (Figure 2). The grain size distributions of soil A1 and C1 match those of soil 1 and soil 6 from the Monteforte Irpino test site. The grain size distribution of soil A2 differs from that of soil 2 be-

cause of the higher fraction of pumeces present in A2.

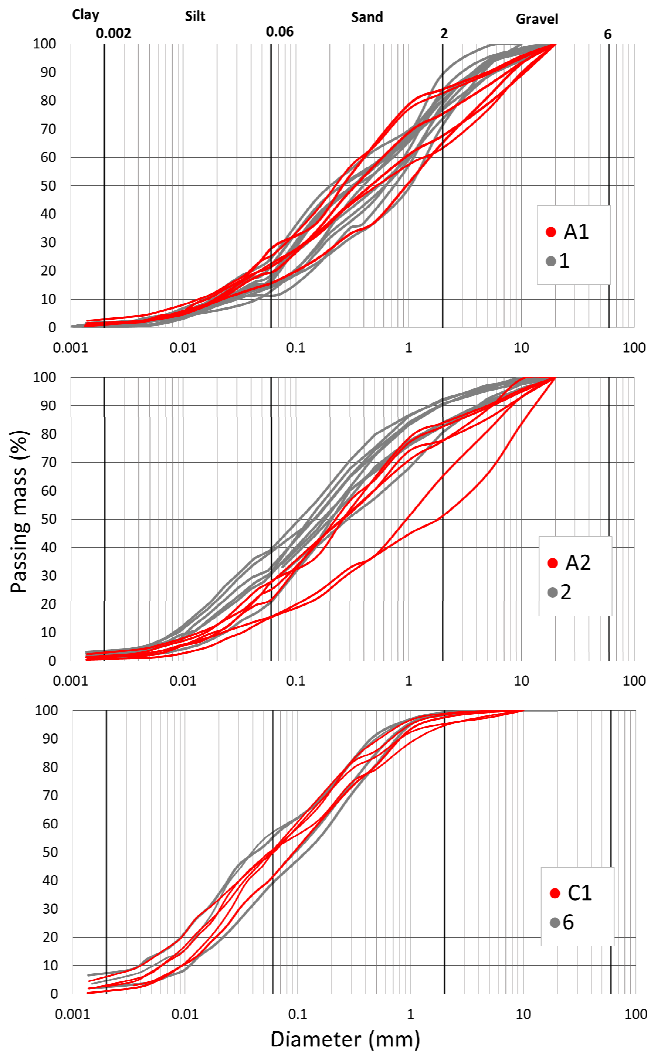


Figure 2. Grain size distribution of soils A1, A2 and C1 from Mount Faito and soils 1, 2 and 6 from Monteforte Irpino.

The physical properties of the soil sampled both at the Mount Faito and Monteforte test sites are summarized in Table 1, in which high values of porosity, typical of pyroclastic soils, can be observed.

Table 1. Mean soil physical properties of Mount Faito (A1, A2 and C1) and of Monteforte (1, 2 and 6 in Pirone et al., 2015a).

Soil	A1	1	A2	2	C1	6
Specific gravity	2.580	2.65	2.688	2.66	2.666	2.57
Dry density ( $\text{g/cm}^3$ )	0.857	0.821	0.804	0.792	0.648	0.727
Porosity	0.668	0.69	0.701	0.70	0.757	0.72

## 4 MATERIALS AND METHODS

### 4.1 Soil samples

Moulds of PVC with an internal diameter of 19.2 cm were horizontally inserted into the soil in a trench at the test site to collect undisturbed soil samples. Later a plexiglas base was attached to the mould (Figure 3).



Figure 3. Setup of instrumentation.

The amount of collected soil is variable and is indicated in Table 2, as well as dry density and porosity values of the tested samples.

Table 2. Properties of the tested samples.

Soil	A1	A2	C1
Sample height (cm)	22.2	15.7	20.8
Dry density ( $\text{g/cm}^3$ )	0.746	0.857	0.612
Porosity	0.711	0.681	0.758

### 4.2 Equipment

The TDR probes used in the experiments were manufactured with the dimensions presented in Figure 4. The rods are 15 cm long, with a diameter of 0.5 cm and spaced by 3.2 cm. The most similar standard probe to the ones used in this experiment is the CS630 3-rod probe.

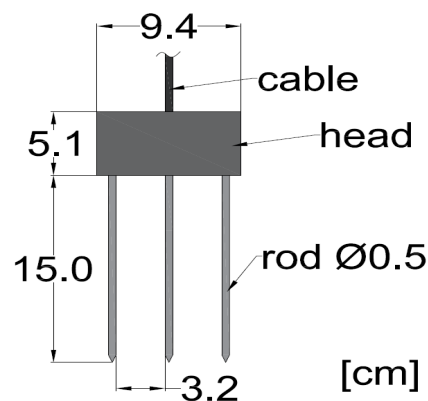


Figure 4. TDR probe dimensions.

A calibration of the probe constants was made according to the procedure suggested by the software PCTDR 3.0 by Campbell Scientific, Inc. because the probes used in this experiment were not standard. These constants are required by the PCTDR software for the interpretation of the recorded signal. The probes constants resultant from this calibration are presented in Table 3, where the "calibration probe length" refers to the rods length and the "calibration probe offset" is a parameter used to correct the effect of the probe head on the measurements.

Table 3. Mean probe constants.

Calibrated probe length (m)	0.1543
Calibrated probe offset	0.0611

### 4.3 Experimental procedure

The samples were saturated by adding distilled water. The weight of the samples was controlled to guarantee that enough water had been added to reach saturation. A negative pressure, approximately 10 kPa, was applied to the top of the sample to remove remaining air in the soil voids. This pressure was applied by sealing the sample with a plastic cap and connecting it to a vacuum pump.

The TDR probe was inserted vertically into the soil. Tests were performed on the samples during drying and wetting phases. In the drying phase, the water was lost through evaporation. Periodically, the weight and the dielectric constant of the samples were measured. In the wetting phase, distilled water was added to saturate the samples in 6 steps. The weight and dielectric constant were measured concurrently every 24 hours to allow the water to diffuse into the soil samples. No settlements were observed during the experiment.

At the end, the samples were dismantled and the porosity was determined to estimate the value of volumetric water content ( $\theta$ ) based on the weight of the samples measured during the tests.

## 5 RESULTS AND DISCUSSION

Couples of measured dielectric constant and volumetric water content of all the soils tested (A1, A2 and C1) are presented in Figure 5. Measurements are not affected by paths, wetting or drying, and results seem indistinguishable for all the soils. However, measurements start to differ for water contents higher than 0.5. The sample A2 presents higher dielectric constant values for the same water content when compared with A1 and C1. Figure 5 also shows that the popularly used calibrations curves (Topp and Ledieu equations) underestimate the volumetric water content.

Table 4. Calibration parameters of the polynomial model.

Soil	a·10 <sup>-6</sup>	-b·10 <sup>-4</sup>	c·10 <sup>-2</sup>	d·10 <sup>-2</sup>	R <sup>2</sup>
A1	6.450	6.424	2.935	4.541	0.9817
A2	4.132	5.748	2.986	1.500	0.9889
C1	9.296	8.609	3.310	2.239	0.9831

Table 5. Calibration parameters of the logarithmic model.

Soil	a	b	R <sup>2</sup>
A1	-0.2547	0.2304	0.9756
A2	-0.2098	0.2069	0.9846
C1	-0.3008	0.2383	0.9579

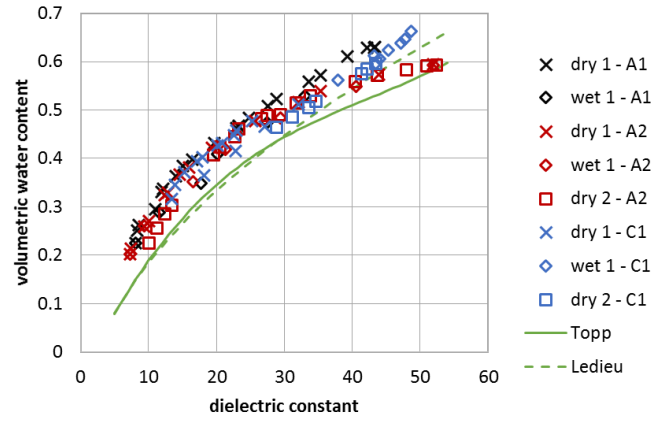


Figure 5. Couple of measured dielectric constant and correspondent volumetric water content.

The calibration parameters of Equations 5 to 7 were fitted to the data, whose values are presented in Tables 4 to 6. The  $R^2$  index that provides an indication of the quality of the fitting is also presented in these Tables. The model that best fitted data was the polynomial. The curves correspondent to the polynomial, logarithmic and Roth models are presented in Figure 6. The poor fitting of the Roth model to the experimental data may be due to: (1) the incorrect estimation of the solid particles dielectric constant ( $\epsilon_s$ ) because volcanic soil presents higher  $\epsilon_s$  values than other soils, as previously mentioned; or (2) lack of distinction of the dielectric constants of absorbed and free water, which is considered in the 4-phase models.

Table 6. Calibration parameters of the Roth model.

Soil	$\epsilon_s$	$\alpha$	R <sup>2</sup>
A1	4.54	0.425	0.9813
A2	4.75	0.428	0.9550
C1	4.44	0.558	0.9826

Also in Figure 6, experimental data were compared with relations provided by Papa and Nicotera (2012), the polynomial (poly), logarithmic (log) and Roth functions (Roth). It is worth to note that the Authors collected experimental data of Monteforte test site soils up to a volumetric water contents close to 0.50. Therefore, their calibration functions extrapolate estimations for  $\theta$  greater than 0.50. Definitely, the calibration functions by Papa and Nicotera (2012): (i) underestimate the volumetric water content in soil A1 (except the Roth function); (ii) match well the experimental data of soil A2 and C1 for  $\theta$  lower than 0.50. Moreover, the logarithmic functions fit satisfactorily the data over all the range of values. It is important to stress that the polynomial model performs well when the dielectric constant is lower than 30 ( $\theta$  lower that 0.5), after which the estimated values are extrapolated, justifying their deviation from the experimental points.

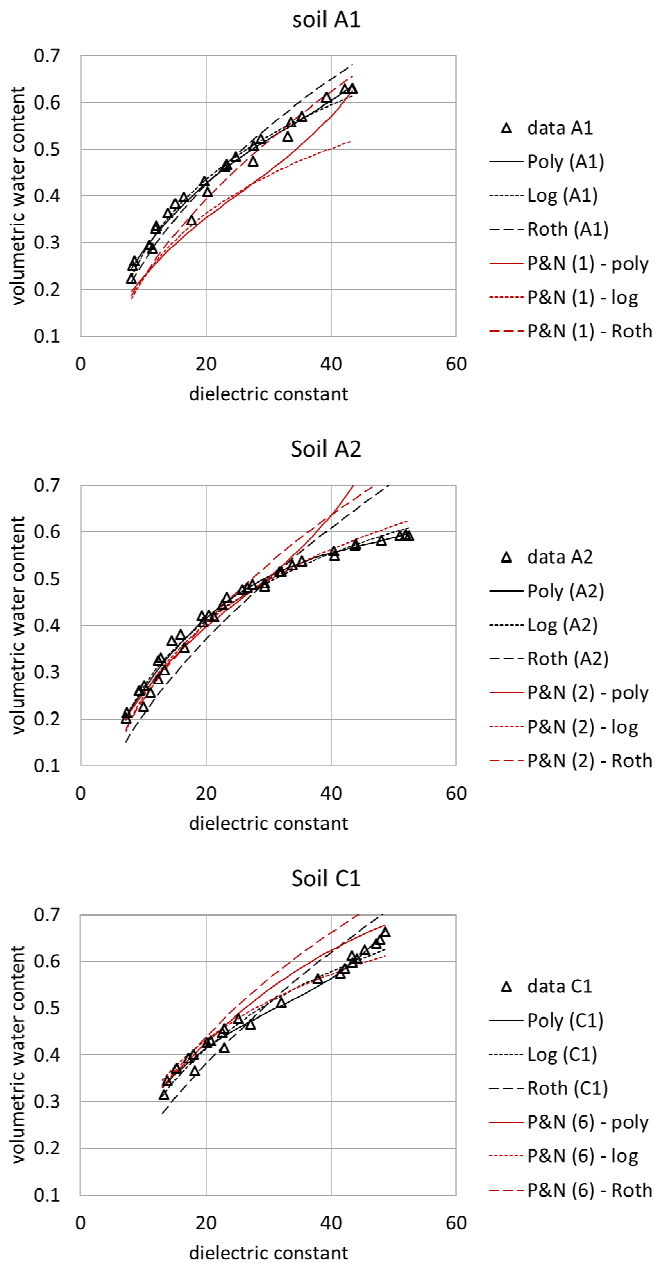


Figure 6. Fitting of experimental data with equations available in the literature and comparison to the calibration function obtained by Papa and Nicotera (2012).

## 6 CONCLUSIONS

The following conclusions can be drawn:

- Topp and Ledieu equations underestimate the volumetric water content of pyroclastic soils;
- Roth model performs unsatisfactory in comparison with the polynomial and the logarithmic model;
- The less satisfactory performance of the Roth model may be caused by a poor estimation of the dielectric constant of the solid particles or by not differentiating the dielectric constants of free and adsorbed water;
- The polynomial model presented the best performance, as it is confirmed by the high  $R^2$

index, and for this reason it is recommended for TDR calibration;

- The soils 2 and 6, studied by Papa and Nicotera (2012), present similar behaviour to soils A2 and C1, respectively, up to a value of  $\theta$  close to 0.50;
- The use of the polynomial model constants provided by Papa and Nicotera (2012) are recommended up to values of  $\theta$  close to 0.50.

## 7 ACKNOWLEDGEMENTS

The authors wish to acknowledge the support of the European Commission via the Marie Skłodowska-Curie Innovative Training Networks (ITN-ETN) project TERRE ‘Training Engineers and Researchers to Rethink geotechnical Engineering for a low carbon future’ (H2020-MSCA-ITN-2015-675762).

## 8 REFERENCES

- Comegna, A., Coppola, A., Dragonetti, G., Severino, G., Sommella, A., & Basile, A. 2013. Dielectric properties of a tilled sandy volcanic-vesuvian soil with moderate andic features. *Soil & Tillage Research* 133: 93-100.
- De Vita, P., Agrello, D., & Ambrosino, F. 2006. Landslide susceptibility assessment in ash-fall pyroclastic deposits surrounding Mount Somma-Vesuvius: Application of geophysical surveys for soil thickness mapping. *Journal of Applied Geophysics* 59(2): 126-139.
- Dobson, M.C., Ulaby, F.T., Hallikainen, M.T., & El-Rayes, M.A. 1985. Microwave dielectric behavior of wet soil-Part II: Dielectric mixing models. *IEEE Transactions on Geoscience and Remote Sensing* 1: 35-46.
- Frattini, P., Crosta, G.B., Fusi, N., & Dal Negro, P. 2004. Shallow landslides in pyroclastic soils: A distributed modelling approach for hazard assessment. *Engineering Geology* 73(3-4): 277-295.
- Hendrickx, J.M.H., Dam, R.L., Van Borchers, B., Curtis, J., Lensen, H.A., & Harmon, R. 2003. Worldwide distribution of soil dielectric and thermal properties. *Detection and remediation technologies for mines and minelike targets VIII* 5089: 1158-1168.
- Hungr, O., Leroueil, S., & Picarelli, L. 2014. The Varnes classification of landslide types, an update. *Landslides* 11(2): 167-194.
- Ledieu, J., De Ridder, P., De Clerck, P., & Dautrebande, S. 1986. A method of measuring soil moisture by time-domain reflectometry. *Journal of Hydrology* 88(3-4): 319-328.
- Noborio, K. 2001. Measurement of soil water content and electrical conductivity by time domain reflectometry: A review. *Computers and Electronics in Agriculture* 31(3): 213-237.
- Papa, R., & Nicotera, M.V. 2012. Calibration of TDR probes to measure water content in pyroclastic soils. *Unsaturated Soils: Research and Applications*: 107-112.
- Pirone, M., Papa, R., Nicotera, M.V., & Urciuoli, G. 2015a. In situ monitoring of the groundwater field in an unsaturated pyroclastic slope for slope stability evaluation. *Landslides* 12(2): 259-276.
- Pirone, M., Papa, R., Nicotera, M.V., & Urciuoli, G. 2015b. Soil water balance in an unsaturated pyroclastic slope for

- evaluation of soil hydraulic behaviour and boundary conditions. *Journal of Hydrology* 528: 63-83.
- Reder, A., Rianna, G., & Pagano, L. 2014. Calibration of TDRs and heat dissipation probes in pyroclastic soils. *Procedia Earth and Planetary Science* 9: 171-179.
- Roth, K., Schulin, R., Hler, H.F.L., & Attinger, W. 1990. Calibration of time domain reflectometry for water content measurement using a composite dielectric approach. *Water Resources* 26(10): 2267-2273.
- Topp, G.C., Davis, J.L., & Annan, A.P. 1980. Electromagnetic determination of soil water content: Measurements in coaxial transmission lines. *Water Resources Research* 16(3): 574-582.
- Urciuoli, G., Pirone M., Comegna L., & Picarelli L. 2016. Long-term investigations on the pore pressure regime in saturated and unsaturated sloping soils. *Engineering Geology* 212: 98-119.